Published in final edited form as:
Circ Arrhythm Electrophysiol. 2012 August 1; 5(4): 640–649. doi:10.1161/CIRCEP.111.970095.

Contribution of Fibrosis and the Autonomic Nervous System to Atrial Fibrillation Electrograms in Heart Failure

Hemantha Koduri, MD[*], **Jason Ng, PhD**[*], **Ivan Cokic, MD**[*], **Gary L. Aistrup, PhD**, **David Gordon, MD, PhD**, **J. Andrew Wasserstrom, PhD**, **Alan H. Kadish, MD**, **Richard Lee, MD**, **Rod Passman, MD**, **Bradley P. Knight, MD**, **Jeffrey J. Goldberger, MD**, and **Rishi Arora, MD**
Feinberg Cardiovascular Research Institute, Northwestern University-Feinberg School of Medicine, Chicago, IL

Abstract

Background—Fibrotic and autonomic remodeling in heart failure (HF) increase vulnerability to atrial fibrillation (AF). Since AF electrograms (EGMs) are thought to reflect underlying structural substrate, we sought to: a) determine differences in AF-EGMs in normal versus HF atria and b) assess how fibrosis and nerve-rich fat contribute to AF-EGM characteristics in HF.

Methods and Results—AF was induced in 20 normal dogs by vagal stimulation and in 21 HF dogs (subjected to 3 weeks of rapid ventricular pacing at 240/min). AF-EGMs were analyzed for dominant frequency (DF), organizational index (OI), fractionation intervals (FI) and Shannon's entropy (ShEn). In 8 HF dogs, AF-EGM correlation with underlying fibrosis/fat/nerves was assessed. In HF, compared to normals, a) DF was lower and OI/FI/ShEn were greater. DF/FI were more heterogeneous in HF. %fat was greater, and fibrosis and fat more heterogeneously distributed in the posterior left atrium (PLA) than left atrial appendage (LAA). DF/OI correlated closely with %fibrosis. Heterogeneity of DF/FI correlated with heterogeneity of fibrosis. Autonomic blockade caused a greater change in DF/FI/ShEn in the PLA than LAA, with the decrease in ShEn correlating with %fat.

Conclusions—The amount and distribution of fibrosis in the HF atrium appears to contribute to slowing and increased organization of AF-EGMs, while the nerve-rich fat in the HF-PLA is positively correlated with AF-EGM entropy. By allowing for improved detection of regions of dense fibrosis and high autonomic nerve density in the HF atrium, these findings may help enhance the precision and success of substrate-guided ablation for AF.

Keywords

atrium; fibrillation; heart failure; nervous system; autonomic; fibrosis

Introduction

Atrial fibrillation (AF) is a complex arrhythmia, with a variety of underlying molecular and structural mechanisms contributing to a vulnerable AF substrate[1, 2]. The complexity of AF

Correspondence: Rishi Arora, MD, Northwestern University-Feinberg School of Medicine, 251 East Huron, Feinberg 8-503, Chicago, IL 60611, Tel: 312-503-3217, Fax: 312-926-6295, r-arora@northwestern.edu.
[*]contributed equally as co-first authors

Conflict of Interest Disclosures: None

substrate appears to be reflected in the characteristics of AF electrograms (EGMs), with AF-EGM morphology in paroxysmal AF being different than in more persistent AF[3]. However, the precise structural and functional mechanisms that lead to the formation of AF EGMs have not been well elucidated. The need for a better understanding of the mechanisms underlying AF EGM formation is heightened by several recent descriptions of regions of high frequency activity during AF, called complex fractionated atrial EGMs (CFAEs).[4] Several recent reports suggest that ablation of CFAEs appears to increase AF ablation success[5].

In the setting of structural heart disease, specifically HF, a variety of mechanisms e.g. changes in ion-channel expression and gap junction distribution, inflammation, oxidative stress, and a variety of structural changes are thought to contribute to the creation of a vulnerable AF substrate[2]. Of the structural changes that occur in the HF atrium, fibrosis is considered to be especially important in creating conditions conducive to the genesis and maintenance of AF[2]. In more structurally 'normal' hearts, other mechanisms e.g. heightened autonomic activity[6] are thought to play a more dominant role in the genesis of AF. We therefore postulated that time and frequency domain characteristics of AF EGMs would be significantly different during AF recorded from a canine HF model of AF (a model that is known to harbor a large amount of fibrosis)[7] as compared to AF induced in normal dogs with autonomic stimulation. We further hypothesized that the signal content AF EGMs in HF would be closely correlated with the extent and heterogeneity of fibrosis (and the related distribution of fat and myocardium). Specifically, we hypothesized that increasing fibrosis would correlate with slowing and disorganization of AF-EGMs, and that the spatial distribution (heterogeneity) of fibrosis would directly correlate with spatial distribution of AF-EGMs. Lastly, since autonomic remodeling is known to contribute at least partially to the creation of AF substrate in the setting of HF[8], we hypothesized that the response to autonomic blockade of AF EGMs in the HF atrium would correspond to the underlying distribution of ganglion-rich fibrofatty tissue.

Methods

Detailed methods have been provided for each of the below sections in the Data Supplement.

Experimental Protocol

Purpose-bred hound dogs (weight range: 25-35 kg) were used in this study for both control and HF groups. This protocol conforms to the Guide for the Care and Use of Laboratory Animals published by the U.S. National Institutes of Health (NIH Publication No. 85-23, revised 1996) and was approved by the Animal Care and Use Committee of Northwestern University. Before undergoing the procedures listed below, all animals were premedicated with acepromazine (0.01-0.02 mg/kg) and were induced with propofol (3-7 mg/kg). All experiments were performed under general anesthesia (inhaled) with isoflurane (1-3%). Adequacy of anesthesia was assessed by toe pinch and palpebral reflex.

Canine HF model—In 21 dogs, HF was induced by 3-4 weeks of right ventricular tachypacing (240 bpm) by an implanted pacemaker . In 19 dogs, a transvenous pacemaker was placed via a jugular approach, under aseptic conditions. In 2 dogs, a pacemaker was placed on the ventricle via an epicardial approach (i.e. via a left lateral thoracotomy). Left ventricular function was assessed during pacing by serial echocardiograms[8] (Supplemental Figure 1). HF was confirmed after 3-4 weeks of pacing[8]. Twenty dogs without rapid ventricular pacing were used as controls.

Open-chest mapping—At the terminal study, a left lateral thoracotomy was performed. Low density and high density mapping protocols were used. See the Data Supplement for detailed methods for this section.

AF induction—See the Data Supplement for detailed methods for this section.

Histology

The histologic analysis described below (e.g. comparison of tissue make-up between PLA and LAA) and EGM-tissue analysis was only performed for HF atria, as these atria are known to harbor significant fibrosis. Normal atria on the other hand are not known to have significant fibrosis. Supplemental Figure 2 shows examples of histology from the PLA and LAA of two normal dogs; as shown, there is significantly less fibrosis (blue stain) in normal hearts as compared to HF hearts (see Results).

See the Data Supplement for detailed methods for this section.

EGM Analysis

Custom analysis tools developed in MATLAB (Mathwork, Natick, MA) were used for all offline EGM analysis. The signals were divided into 4 second segments to account for any variability of the both the signals and the measurements of the signals. We have previously shown that dominant frequencies averaged from multiple 4-second segments were a better reflection of activation rates than single segments of any length.[9, 10] The following four measurements were computed: Dominant Frequency (DF), Organization Index (OI), Fractionation Interval (FI) and Shannon's Entropy (ShEn). See the Data Supplement for detailed methods for this section.

Tissue Analysis

See the Data Supplement for detailed methods for this section.

Tissue and Electrogram Correlation—Each tissue section was divided into four quadrants. The high density recordings, after being aligned to underlying tissue orientation, were also divided into four quadrants (see schematic in Figure 1B). In each quadrant, the absolute amount of fat, fibrosis and myocardium was assessed. Linear regression analysis was performed to assess the correlation between tissue and EGM characteristics.

Statistical Methods

All data is reported as mean±standard error. Mixed effects ANOVA was used to compare the mean DF, OI, FI and ShEn between HF and normal dogs and between PV, PLA, and LAA. Standard deviations to quantify spatial heterogeneity were also analyzed in a similar fashion. In the HF dogs that underwent high-density mapping, comparison of EGMs between the PLA and LAA were made using unpaired t-tests (as these regions were mapped at separate times during the electrophysiological study i.e. not simultaneously as was the case with low density mapping). Comparisons of tissue characteristics between the PLA and LAA were made using paired t-tests. Before and after comparisons made in same animals (e.g., before and after double autonomic sblockade) were assessed for significant differences via paired t-tests.

Tissue and EGM correlations were performed by dividing each tissue section into four quadrants paired with the EGM characteristics (DF, OI, FI, and ShEn) of the high density maps similarly divided into four quadrants and performing linear regression analysis.

A p value of ≤ 0.05 was taken as significant for all the above analyses.

Results

AF EGMs in HF versus normal left atrium

Dominant Frequency—Mixed effect ANOVA showed significantly lower mean DFs with HF than in normals ($p=0.0002$) but no significant difference in mean DF between sites ($p=0.65$) (Figure 2A). Heterogeneity (SD) of DF was also lower in HF than in normals, but with significant regional differences (i.e. dispersion) within the left atrium ($p=0.0007$) (Figure 2B). SD of DF for normals was significantly higher in PV than in the PLA and LAA ($p<0.01$), while SD of DF of the PV and PLA were significantly higher than the LAA with HF ($p<0.02$).

Organization index—Mean OI was significantly higher in HF dogs than in normals ($p=0.0001$) with significant regional differences within the left atrium ($p=0.0002$) (Figure 2C). For normal dogs, the OIs were lower in the PLA than in the LAA ($p<0.03$). For HF dogs, the OIs were lower in the PV and PLA than in the LAA ($p<0.04$). SD of OI was not different between HF and normals ($p=0.59$), but showed regional differences within the left atrium (Figure 2D). SD of OI was significantly higher in the PLA than in the LAA ($p<0.002$).

Fractionation index—Mean FI was significantly higher in HF dogs than in normals ($p<0.0001$) with significant regional differences within the left atrium ($p=0.003$) (Figure 2E). For normal dogs, the FIs were significantly lower in the PV and PLA than in the LAA ($p<0.03$). SD of OI was significantly lower in the HF dogs than in the normal dogs ($p<0.0001$), but showed no significant regional differences within the left atrium (Figure 2F).

Percentage (%) of CFAEs—%CFAE was significantly lower in HF than in normals in the PV (72±4 vs. 88±4%, $p=0.002$), PLA (59±4 vs. 92±2%, $p<0.001$) and LAA (59±5 vs. 80±6%, $p=0.003$). In HF, %CFAE was significantly greater in the PV than in the PLA or LAA ($p<0.05$ for both comparisons). In normals, %CFAEs were significantly greater in the PLA and PV than in the LAA ($p<0.05$ for both comparisons).

Shannon's entropy—Mean ShEn trended lower in HF dogs than in normals ($p<0.08$) with significant regional differences within the left atrium ($p=0.003$) (Figure 2G). For HF dogs, ShEn were significantly higher in the PV and PLA than that in the LAA ($p<0.0006$). SD of ShEn was not different between HF dogs and normal dogs ($p=0.14$) or between sites ($p=0.31$) (Figure 2H).

AF EGM characteristics in the HF PLA vs. LAA (with high-density plaques)

In both the PLA and LAA, there was no difference in DF between low and high-density plaques (see Supplemental Figure 3). However, OI was lower, FI was greater and ShEn was lower with high-density plaques as compared to the low-density plaques (Supplemental Figure 3). This is likely due to the difference in inter-electrode distance between the plaques; as shown in the Supplemental Data Figure 4, increasing inter-electrode distance for the same set of bipolar recordings results in a decrease in OI, decrease in FI and increase in ShEn. All the remaining AF mapping data below was obtained with high-density plaques. In the one dog that underwent both low and high density mapping, the differences between low and high density mapping were consistent with the overall mean differences for all dogs between low vs high density mapping (see Supplemental Table 1).

Overall, differences between the PLA and LAA during high-density mapping (where the PLA and LAA were mapped sequentially) were similar to those found during low-density

mapping (where the PV, PLA and LAA were mapped simultaneously). OI was significantly lower in the HF PLA as compared to the LAA, with ShEn trending towards being greater in the PLA than in the LAA (Figure 3A). DF, OI, FI and ShEn were all more heterogeneous in the HF PLA than the LAA (Figure 3B).

Distribution of fibrosis, fat and nerves in the HF left atrium

The PLA had significantly more fat than the LAA (36.4±2.8 vs. 21.6±2.2% ($p<0.001$) (Figure 4A, subpanel i). % myocardium was greater in the LAA than in the PLA (53.5±2.4 vs. 35.6%±2.9%, $p<0.001$). There was no significant difference in fibrosis between the PLA and LAA. % fat was assessed in the PLA in a small number of normal dogs (N=3), and was found to be no different than in HF (36.4±2.8 vs 30.1±2.1%, $p=0.22$).

Myocardium and fibrosis were more heterogeneously distributed in the PLA than in the LAA (SD of % myocardium in PLA vs. LAA = 20.5±1.7 vs. 14.1± 1.3%, $p=0.01$; SD of % fibrosis in PLA vs LAA = 16.9±1.9 vs 12.3±1.5, $p=0.02$). (Figure 4A, subpanel ii). Fat also trended towards being more heterogeneous in the PLA than in the LAA (17.3±1.7 vs. 12.3±2.3%, $p=0.07$).

Figure 4B shows examples of significantly greater fat in the PLA (subpanels i and iii) than the LAA (subpanels ii and iv). These panels also demonstrate that fat, fibrosis and myocardium were more heterogeneously distributed in the PLA than in the LAA. A significant number of nerve trunks were noted in the PLA fat (43±9) (see Figure 4B, subpanel i and Figure 7C for examples of nerve trunks/bundles in the PLA). In contrast, no nerve trunks were found in the LAA.

Correlation between AF EGM characteristics and fibrosis

DF was negatively correlated to % fibrosis ($r = -0.45$, $p=0.006$, Figure 5A, subpanel i), while FI was positively correlated with % fibrosis ($r = 0.42$, $p=0.01$) (Figure 5A, subpanel ii) in the PLA. Heterogeneity (SD) of DF and heterogeneity (SD) of FI were correlated with heterogeneity (SD) of fibrosis (for DF, $r = 0.41$, $p=0.01$; for FI, $r = 0.47$, $p = 0.004$) (Figure 5B, subpanels i and ii respectively).

Figure 6A shows an example of OI being lower and more heterogenous (i.e. greater SD) in the HF PLA than the LAA. Figure 6B shows an example of DF being more heterogeneous in the HF PLA as compared to the LAA. Subpanels i and ii in each panel show the Masson-Trichrome stained PLA and LAA respectively. Subpanels iii and iv in figure 6A show the corresponding OI maps for each region mapped. Similarly, subpanels iii and iv in figure 6B show the corresponding DF maps for each region mapped.

Effect of double autonomic blockade on EGM content in the HF left atrium

In the PLA double autonomic blockade lead to a significant decrease in DF (from 6.8±0.6 to 6.1± 0.7 Hz, $p<0.001$) and an increase in FI (from 138±18 to 158±26 ms, $p=0.002$) (Figure 7A). The increase in FI by double autonomic blockade was paralleled by a decrease in % CFAEs in the PLA (from 34±15 to 21±13%, $p=0.01$). A trend towards decrease of ShEn was noted in PLA in the presence of double autonomic blockade (from 0.76±0.01 to 0.73±0.01, $p=0.098$). No change in OI was noted in the PLA with double autonomic blockade. In the LAA, there was no change in any of these measures in the presence of double autonomic blockade (Figure 7A). Figure 7B shows examples of EGMs before and after autonomic blockade; as shown, the AF-EGMs become significantly slower and less fractionated after autonomic blockade. Figure 7C shows that with autonomic blockade, DF changes significantly over regions of fat in the PLA. In figure 7C, subpanels i shows the PLA being mapped. Subpanels ii and iii show the DF map before and after autonomic blockade; as

shown, there is a significant decrease in DF after autonomic blockade. Moreover, the decrease in DF is most pronounced over regions of fat that contain large nerve trunks (encircled regions). Subpanel iv highlights a large nerve trunk seen in subpanel i.

In the PLA, change in ShEn (ΔShEn) with autonomic blockade was positively correlated with % fatty tissue ($r = 0.42$, $p<0.05$) (Figure 5C).

Discussion

In this study, we have systematically assessed the correlation between AF EGM characteristics and the underlying quantity and distribution of fibrosis. Using a variety of time and frequency domain measures, we examined the signal characteristics of AF EGMs in the setting of HF (where fibrosis is known to be a key contributor to the genesis and maintenance of AF) and compared these with AF EGMs in normal hearts (where AF was induced by vagal stimulation). We also systematically assessed the relationship between the characteristics of AF EGMs in HF and the underlying distribution of myocardium, fibrosis, fat and autonomic ganglia in the failing left atrium. Our findings are summarized as follows: 1) AF EGM measures are significantly different in AF in the normal vs. the HF atrium, with AF being slower (lower DF), more organized (higher OI) and having a higher FI in the setting of HF, 2) there are significant regional differences in AF signal content in HF, with AF being less organized (lower OI) in the PLA than in the LAA; moreover, all EGM measures are significantly more spatial heterogeneous in the PLA than in the LAA, 3) there is a significantly greater amount of fat in the PLA as compared to the LAA, with the fat being richly innervated with large nerve trunks; moreover, fibrofatty tissue is more heterogeneously distributed in the PLA than in the LAA, 5) AF signal content in the HF atrium correlates with the total amount of fibrosis, with increasing fibrosis correlating with slowing and increased organization of AF EGMs; furthermore, heterogeneity of AF signal content in the HF atrium correlates with the heterogeneity of underlying fibrosis, 6) autonomic blockade significantly decreases DF and increases FI (with a resulting decrease in CFAEs) in the PLA, and 7) the autonomic responsiveness of AF EGMs (i.e. entropy of AF signals) is directly correlated with the amount of nerve-rich fatty tissue present in the myocardium.

Differences in AF EGM characteristics in HF vs. normal heart – contribution of fibrosis to AF EGMs

While animal and clinical studies strongly suggest that fibrosis and other structural changes in the myocardium contribute to substrate for sustained AF[2], the precise contribution of fibrosis to EGM characteristics in AF is not well characterized. However, recent studies do suggest that there are differences in the distribution and characteristics of CFAEs in paroxysmal and permanent AF[3, 11]. These differences may at least be in part due to the heterogeneity of underlying structural substrate in these patients, with atria in persistent AF being more likely to harbor fibrotic changes[12]. It is known that slow or heterogeneous conduction[13, 14] can lead to the formation of fractionated EGMs e.g. as seen in infarcts after a period of healing[14], with electrical uncoupling of fibers occurring at the microscopic level resulting in complex pathways and zig-zag propagation. A similar scenario may occur in the presence of fibrous tissue[15]. In this study, we have attempted to systematically characterize AF EGMs in two well characterized substrates for AF i.e. a) in a normal heart where vagal stimulation (with resulting refractory period shortening) is the primary mechanism for AF and b) in pacing-induced HF, where fibrosis is thought to be a dominant mechanism underlying AF[7], with other mechanisms such as oxidative stress[16] and autonomic dysfunction[8] also contributing at least partially to AF substrate. We discovered that AF EGM content is significantly different in normal vs. HF atria, with EGMs in HF being significantly slower, and contrary to our initial hypothesis, more organized and less

fractionated as compared to AF EGMs in normal hearts. The strong correlation between the amount and heterogeneity of fibrosis and the time and frequency domain measures of AF EGMs in HF suggests that fibrosis may be at least partially contributing to AF EGM characteristics. These findings also suggest that in patients with AF, worsening structural heart disease may be contributing not just to the increasing chronicity of AF but also to AF EGM content. While these findings may seem contradictory to clinical data that shows that CFAE% are higher in patients with persistent than in paroxysmal AF[17], it must be remembered that the precise structural substrate underlying AF EGMs (and the specific contribution of fibrosis to AF EGMs) was not characterized in these prior studies. Indeed, the observation by Xi et al[18] that f-wave frequency of AF on surface ECGs is known to decrease with increasing age further supports the notion that increasing atrial fibrosis – which is well known to occur in the aging heart – may also be contributing to a slowing and organization of AF in the failing atrium. A possible explanation for our findings may also be the fact that the dogs we studied had fairly advanced HF and a large amount of fibrosis. It is tempting to speculate that lesser degrees of interstitial fibrosis between healthy myocytes e.g. in early stage HF, may be more likely to set up microscopic conduction barriers (and resulting anisotropy) that may be conducive to the creation of disorganized EGMs. However, increasing fibrosis and an accompanying reduction in viable myocardium – as may be seen in advanced HF - may lead to a coalescing and organization of activation wavefronts in the atrium, with an increased organization of AF EGMs. In addition, pacing induced heart failure is known to lead to prolongation of atrial refractoriness[19]; an increase in the atrial ERP causes an increase in AF wavelength and may therefore lead to an increase in the AF cycle length and organization. Further studies need to be done to assess the effect of the severity/stage of HF on AF EGM organization. Another possible explanation for the differences observed in the HF dogs vs normal dogs is that in the latter AF was induced by vagal stimulation. Since true ‘vagal’ AF is seen only in a minority of patients with paroxysmal AF, the normal AF characteristics that we demonstrate in our canine model may not be representative of all patients with paroxysmal AF.

It therefore appears that EGM differences between HF and normal hearts may provide valuable insight into the pathophysiologic mechanisms underlying AF, and may be of potential clinical significance in patients with AF undergoing AF ablation. It is well known that success rates of ablation procedures decrease in patients with permanent AF (as compared to paroxysmal AF), at least in part due to the presence of structural heart disease in these patients[20]. However, the addition of EGM guided ablation (e.g. CFAE ablation) appears to increase long-term success of these procedures[21]. Nonetheless, despite the success of CFAE guided ablation in decreasing AF recurrence in some series, it is well recognized that not all CFAEs contribute to the formation of AF substrate. A better understanding of EGM signal content and how it relates to the underlying areas of fibrosis may therefore help refine current, EGM-based ablation techniques. For example, based on the findings of the current study, the increased regularity of EGMs (indicated by increased OI in HF), in the presence of slower activation rates (indicated by lower DFs and higher FIs) in HF may indicate the presence of regions of underlying fibrosis. It is tempting to speculate that an enhanced ability to identify regions islands of dense fibrosis (by real-time AF-EGM analysis) may in turn allow for a greater precision in the placement of linear ablation lesions in the atrium.

Contribution of the autonomic nervous system to AF EGMs in the HF left atrium

Recent data suggests that at least some left atrial CFAEs may be located in the anatomic vicinity of autonomic ganglionated plexi (GPs).[22, 23] Other data indicates that heightened vagal activity may contribute to the formation of CFAE-like EGMs[22, 24]. More recently, Habel et al[25] showed that CFAEs organize and DF decreases in the atrium in response to

autonomic blockade. Knecht et al[26] also showed that CFAEs organize in response to autonomic blockade, with organization being noted in patients with paroxysmal but not persistent AF. To our knowledge though, the effect of autonomic blockade on AF in the setting of HF has not been well studied. Based on the findings of Knecht et al[26], one would suspect that in the presence of structural heart disease, which is more likely to cause persistent AF, there would be little autonomic contribution to AF EGMs. However, our data clearly demonstrates a decrease in DF and increase in FI in the failing PLA in the presence of autonomic blockade. The present study also demonstrates that autonomic changes in EGM content correlate with the underlying distribution of nerve-rich fibrofatty tissue in the PLA. These diverging results may be partially explained by species differences between persistent human AF and AF in a canine HF model. Nonetheless, the findings of this study are consistent with recent studies that support a role for the autonomic nervous system in contributing to AF substrate in the HF setting[8, 27, 28]. Indeed, both the sympathetic and the parasympathetic nervous system appear to be contributing to AF substrate in HF; [8] in that study, it was reported that inspite of the vagal hyperinnervation noted in the HF left atrium there is a decrease in vagal responsiveness in the HF atria, because of a compensatory increase in acetycholineestrase (ACHE) activity. It is possible that this increase in ACHE activity may be contributing at least partially to the differences noted in AF EGM characteristics in HF AF vs AF induced by vagal stimulation in normal dogs. The enhanced autonomic responsiveness of AF EGMs in the PLA (as compared to the LAA) also supports our recent findings where autonomic remodeling in the HF atrium - both at the structural and functional level - is significantly more pronounced in the PLA than in the rest of the left atrium[8]. Taken together, the clear contribution of fatty tissue harboring large autonomic nerve trunks to time and frequency domain measures of EGM characteristics suggests that a detailed assessment of AF EGM content in the present of autonomic blockade may help better target autonomic ganglia during ablation.

Study limitations

This was an animal study; our results in normal canine hearts (i.e. vagal induced AF) and in the setting of pacing induced HF cannot therefore be directly extrapolated to human AF, both for normal and diseased hearts. Moreover, detailed EGM-tissue correlations were performed only in HF atria, and not in normal atria. Also, AF is a multifactorial disease, and a variety of mechanisms contribute to the creation of AF substrate; in this study, we only examined the contribution of fibrosis and the autonomic nervous system to AF EGM content. Future studies are needed to investigate the contribution of other mechanisms on EGM formation in the HF atrium e.g. fiber orientation, gap junction expression, oxidative stress etc.

Lastly, the correlation between fibrosis distribution and AF EGM content does not necessarily imply a causal role for fibrosis in CFAE formation. Further studies are necessary in order to fully understand how fibrosis contributes to EGM characteristics in AF, both in normal hearts and in the setting of HF.

Since we mapped the epicardium, we only assessed histology from the epicardial aspect of the left atrium. However, due to transmural differences in electrophysiological characteristics in the atrial wall[29], characteristics of AF EGMs mapped epicardially cannot be directly extrapolated to the endocardium. Further studies are needed to assess the impact of transmural tissue characteristics on AF EGMs.

Even though we performed double autonomic blockade in HF, we did not perform parasympathetic blockade alone vs sympathetic blockade alone, in order to study the specific effects of sympathetic vs parasympathetic signaling on AF EGMs in HF.

supplementary-material

Refer to Web version on PubMed Central for supplementary material.

Acknowledgments

Funding Sources: This work was supported by NIH (NHLBI) [1R01HL093490, 3R01HL093490-01S1, R21 HL088304]; and the Everett/O'Connor Trust; and the Dixon Translational Research Award (Northwestern Memorial Hospital).

References

1. Nattel S. From guidelines to bench: Implications of unresolved clinical issues for basic investigations of atrial fibrillation mechanisms. Can J Cardiol. 2011; 27:19–26. [PubMed: 21329858]
2. Nattel S, Burstein B, Dobrev D. Atrial remodeling and atrial fibrillation: Mechanisms and implications. Circ Arrhythm Electrophysiol. 2008; 1:62–73. [PubMed: 19808395]
3. Ciaccio EJ, Biviano AB, Whang W, Gambhir A, Garan H. Different characteristics of complex fractionated atrial electrograms in acute paroxysmal versus long-standing persistent atrial fibrillation. Heart Rhythm. 2010; 7:1207–1215. [PubMed: 20558323]
4. Nademanee K, McKenzie J, Kosar E, Schwab M, Sunsaneewitayakul B, Vasavakul T, Khunnawat C, Ngarmukos T. A new approach for catheter ablation of atrial fibrillation: Mapping of the electrophysiologic substrate.[see comment]. J Am Coll Cardiol. 2004; 43:2044–2053. [PubMed: 15172410]
5. Hayward RM, Upadhyay GA, Mela T, Ellinor PT, Barrett CD, Heist EK, Verma A, Choudhry NK, Singh JP. Pulmonary vein isolation with complex fractionated atrial electrogram ablation for paroxysmal and nonparoxysmal atrial fibrillation: A meta-analysis. Heart Rhythm. 2011; 8:994–1000. [PubMed: 21397045]
6. Chen PS, Tan AY. Autonomic nerve activity and atrial fibrillation. Heart Rhythm. 2007; 4:S61–64. [PubMed: 17336887]
7. Li D, Fareh S, Leung TK, Nattel S. Promotion of atrial fibrillation by heart failure in dogs: Atrial remodeling of a different sort. Circulation. 1999; 100:87–95. [PubMed: 10393686]
8. Ng J, Villuendas R, Cokic I, Schliamser JE, Gordon D, Koduri H, Benefield B, Simon J, Murthy SN, Lomasney JW, Wasserstrom JA, Goldberger JJ, Aistrup GL, Arora R. Autonomic remodeling in the left atrium and pulmonary veins in heart failure: Creation of a dynamic substrate for atrial fibrillation. Circ Arrhythm Electrophysiol. 2011; 4:388–396. [PubMed: 21421805]
9. Ng J, Kadish AH, Goldberger JJ. Technical considerations for dominant frequency analysis. J Cardiovasc Electrophysiol. 2007; 18:757–764. [PubMed: 17578346]
10. Ng J, Kadish AH, Goldberger JJ. Effect of electrogram characteristics on the relationship of dominant frequency to atrial activation rate in atrial fibrillation. Heart Rhythm. 2006; 3:1295–1305. [PubMed: 17074635]
11. Ciaccio EJ, Biviano AB, Whang W, Vest JA, Gambhir A, Einstein AJ, Garan H. Differences in repeating patterns of complex fractionated left atrial electrograms in longstanding persistent atrial fibrillation as compared with paroxysmal atrial fibrillation. Circ Arrhythm Electrophysiol. 2011; 4:470–477. [PubMed: 21536597]
12. Schotten U, Verheule S, Kirchhof P, Goette A. Pathophysiological mechanisms of atrial fibrillation: A translational appraisal. Physiol Rev. 2011; 91:265–325. [PubMed: 21248168]
13. Yamabe H, Morihisa K, Tanaka Y, Uemura T, Enomoto K, Kawano H, Ogawa H. Mechanisms of the maintenance of atrial fibrillation: Role of the complex fractionated atrial electrogram assessed by noncontact mapping. Heart Rhythm. 2009; 6:1120–1128. [PubMed: 19539538]
14. Gardner PI, Ursell PC, Fenoglio JJ Jr, Wit AL. Electrophysiologic and anatomic basis for fractionated electrograms recorded from healed myocardial infarcts. Circulation. 1985; 72:596–611. [PubMed: 4017211]

15. Liu X, Shi HF, Tan HW, Wang XH, Zhou L, Gu JN. Decreased connexin 43 and increased fibrosis in atrial regions susceptible to complex fractionated atrial electrograms. Cardiology. 2009; 114:22–29. [PubMed: 19342855]

16. Kim YM, Guzik TJ, Zhang YH, Zhang MH, Kattach H, Ratnatunga C, Pillai R, Channon KM, Casadei B. A myocardial nox2 containing nad(p)h oxidase contributes to oxidative stress in human atrial fibrillation. Circ Res. 2005; 97:629–636. [PubMed: 16123335]

17. Solheim E, Off MK, Hoff PI, Schuster P, Ohm OJ, Chen J. Characteristics and distribution of complex fractionated atrial electrograms in patients with paroxysmal and persistent atrial fibrillation. J Interv Card Electrophysiol. 2010; 28:87–93. [PubMed: 20386973]

18. Xi Q, Sahakian AV, Frohlich TG, Ng J, Swiryn S. Relationship between pattern of occurrence of atrial fibrillation and surface electrocardiographic fibrillatory wave characteristics. Heart Rhythm. 2004; 1:656–663. [PubMed: 15851236]

19. Stambler BS, Fenelon G, Shepard RK, Clemo HF, Guiraudon CM. Characterization of sustained atrial tachycardia in dogs with rapid ventricular pacing-induced heart failure. J Cardiovasc Electrophysiol. 2003; 14:499–507. [PubMed: 12776867]

20. Verma A. The techniques for catheter ablation of paroxysmal and persistent atrial fibrillation: A systematic review. Curr Opin Cardiol. 2011; 26:17–24. [PubMed: 21099681]

21. Nademanee K, Lockwood E, Oketani N, Gidney B. Catheter ablation of atrial fibrillation guided by complex fractionated atrial electrogram mapping of atrial fibrillation substrate. J Cardiol. 2010; 55:1–12. [PubMed: 20122543]

22. Lin J, Scherlag BJ, Zhou J, Lu Z, Patterson E, Jackman WM, Lazzara R, Po SS. Autonomic mechanism to explain complex fractionated atrial electrograms (cfae). J Cardiovasc Electrophysiol. 2007; 18:1197–1205. [PubMed: 17916143]

23. Katritsis D, Giazitzoglou E, Sougiannis D, Voridis E, Po SS. Complex fractionated atrial electrograms at anatomic sites of ganglionated plexi in atrial fibrillation. Europace. 2009; 11:308–315. [PubMed: 19240108]

24. Oh S, Kong HJ, Choi EK, Kim HC, Choi YS. Complex fractionated electrograms and af nests in vagally mediated atrial fibrillation. Pacing Clin Electrophysiol. 2010; 33:1497–1503. [PubMed: 20636313]

25. Habel N, Muller JG, Znojkiewicz P, Thompson N, Calame J, Calame S, Noori A, Gallo A, Lustgarten DL, Sobel BE, Spector PS. The impact of pharmacologic sympathetic and parasympathetic blockade on atrial electrogram characteristics in patients with atrial fibrillation. Pacing Clin Electrophysiol. 2011; 34:1460–1467. [PubMed: 21883315]

26. Knecht S, Wright M, Matsuo S, Nault I, Lellouche N, Sacher F, Kim SJ, Morgan D, Afonso V, Shinzuke M, Hocini M, Clementy J, Narayan SM, Ritter P, Jais P, Haissaguerre M. Impact of pharmacological autonomic blockade on complex fractionated atrial electrograms. J Cardiovasc Electrophysiol. 2010; 21:766–772. [PubMed: 20132382]

27. Ogawa M, Tan AY, Song J, Kobayashi K, Fishbein MC, Lin SF, Chen LS, Chen PS. Cryoablation of stellate ganglia and atrial arrhythmia in ambulatory dogs with pacing-induced heart failure. Heart Rhythm. 2009; 6:1772–1779. [PubMed: 19959128]

28. Ogawa M, Zhou S, Tan AY, Song J, Gholmieh G, Fishbein MC, Luo H, Siegel RJ, Karagueuzian HS, Chen LS, Lin SF, Chen PS. Left stellate ganglion and vagal nerve activity and cardiac arrhythmias in ambulatory dogs with pacing-induced congestive heart failure. J Am Coll Cardiol. 2007; 50:335–343. [PubMed: 17659201]

29. Burashnikov A, Mannava S, Antzelevitch C. Transmembrane action potential heterogeneity in the canine isolated arterially perfused right atrium: Effect of ikr and ikur/ito block. Am J Physiol Heart Circ Physiol. 2004; 286:H2393–2400. [PubMed: 15148061]

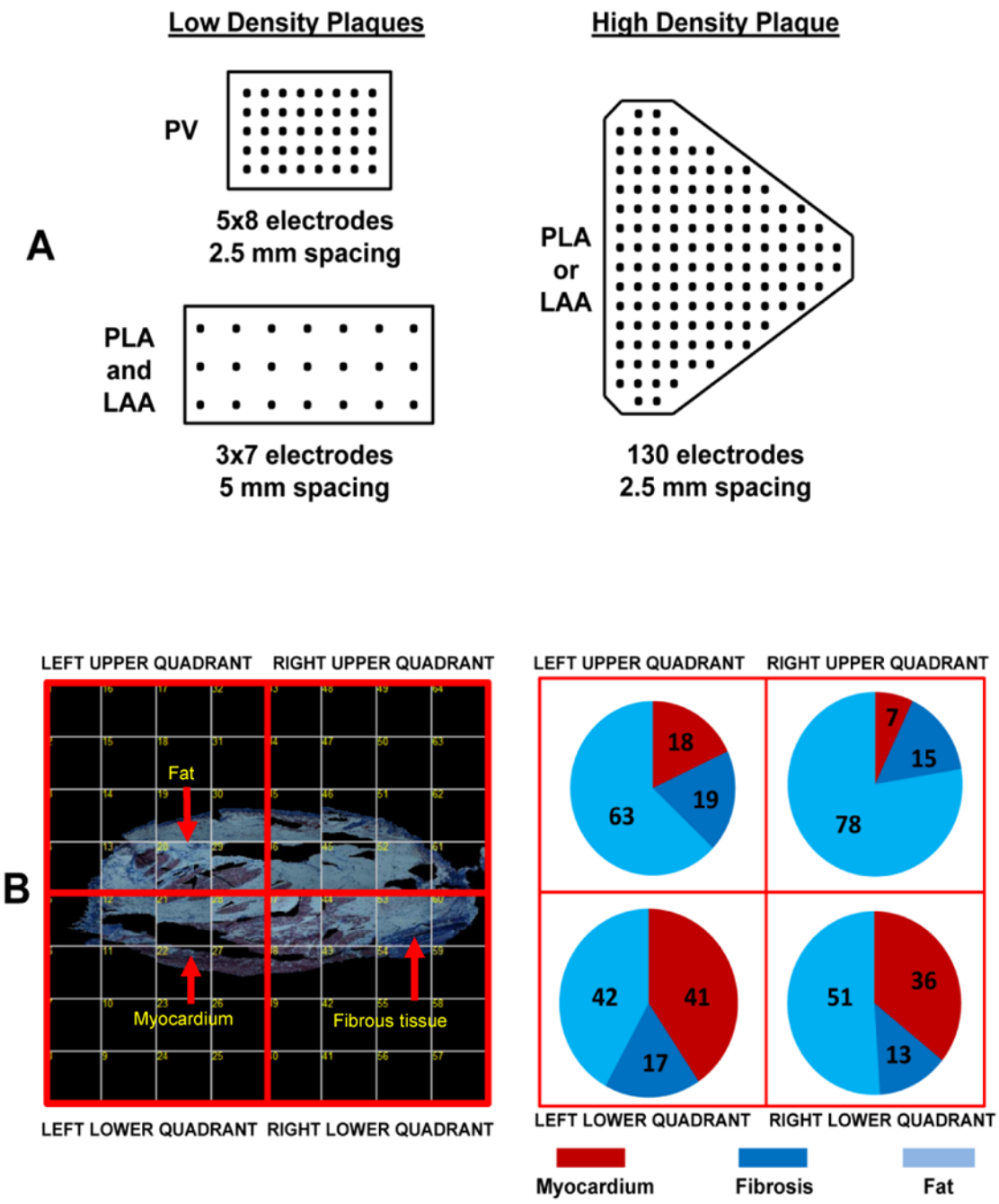

Figure 1.

Panel A shows the density and inter-electrode spacing of the low and high density plaques used for AF-EGM mapping. **Panel B** shows an entire PLA section on the left, composed of several individual photomicrographs at 4X magnification. The panel demonstrates how the PLA section on the left was divided into four quadrants; for each quadrant, tissue composition i.e. % fat vs. myocardium vs. fibrosis was assessed (see subpanel on the right for tissue composition for each quadrant).

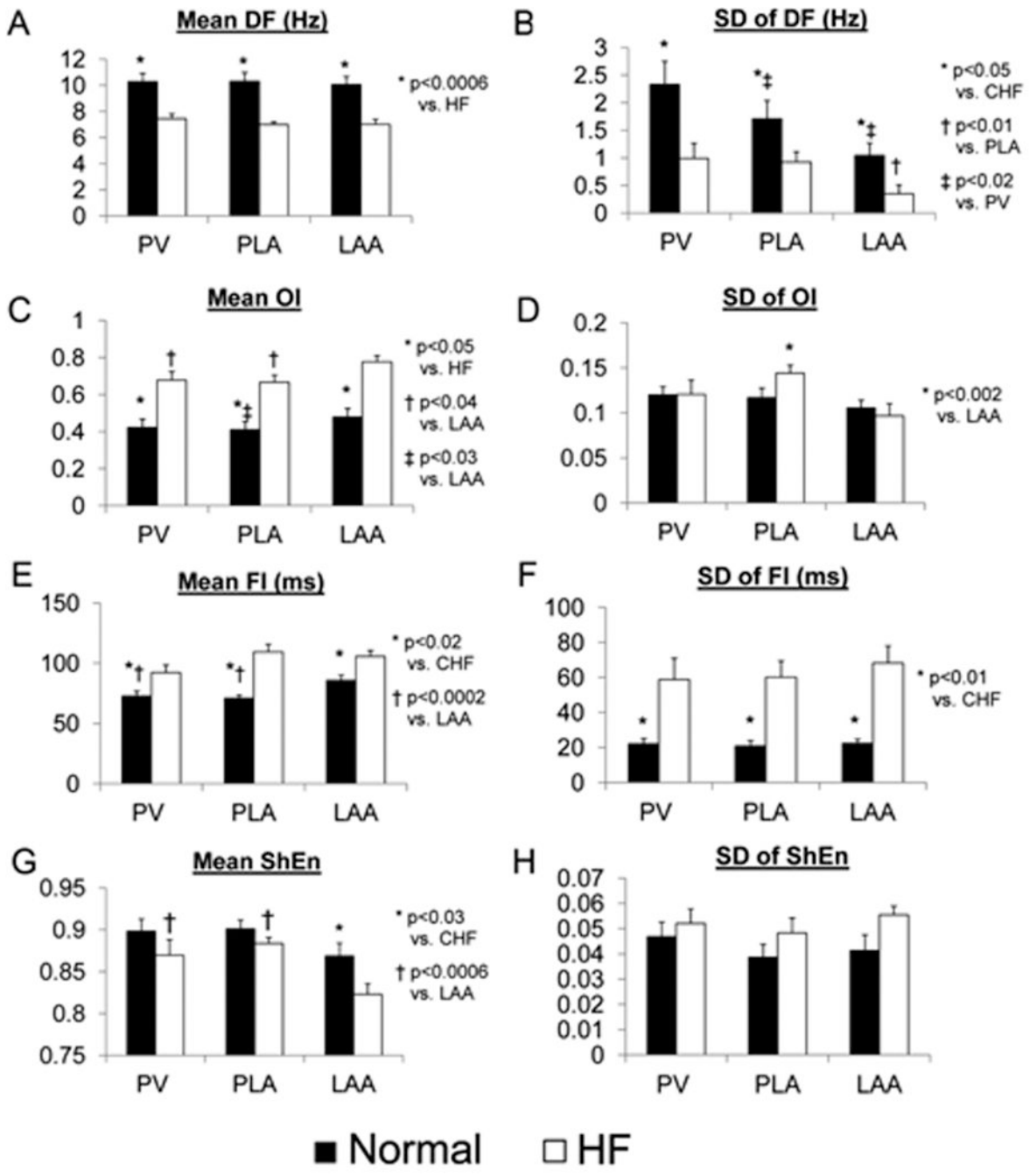

Figure 2.

The figure shows comparisons of DF, OI, FI and ShEn in normal vs. HF atria. Comparisons were made for mean (panels A,C,E,G) and SD (panels B,D,F,H) of each AF measure. Comparisons were made for the PLA, PV and LAA.

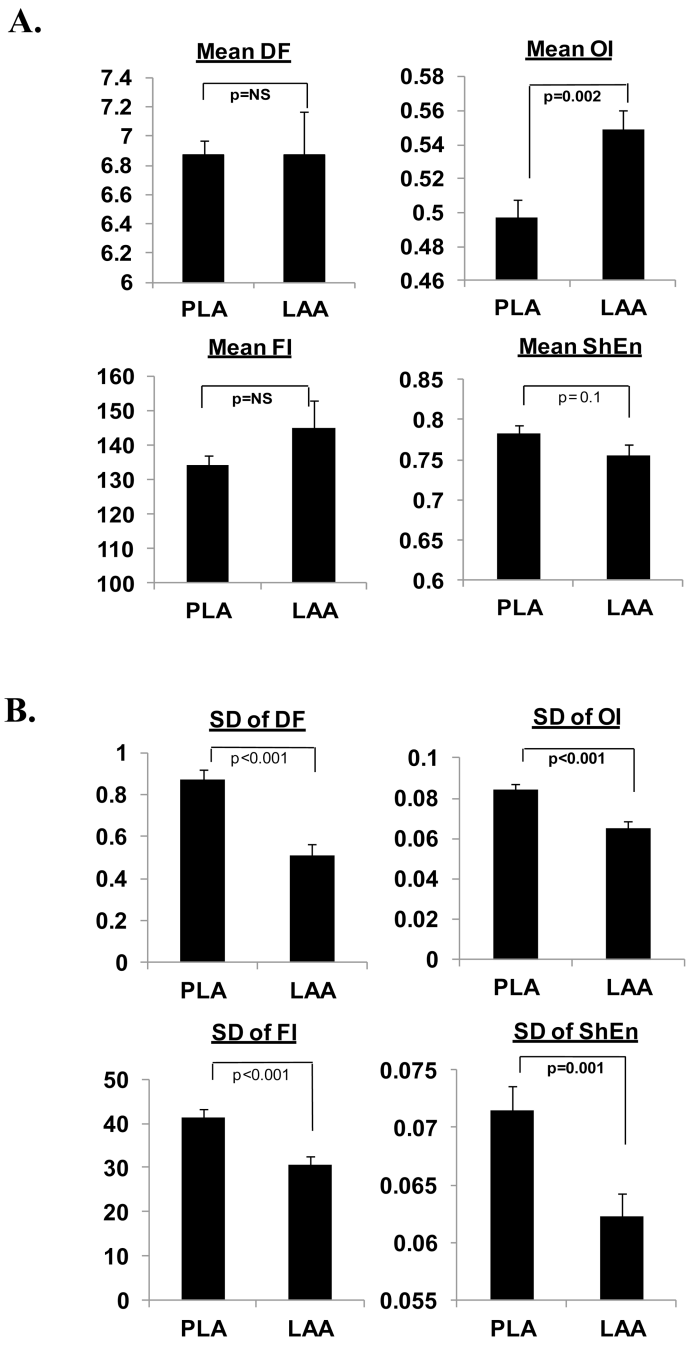

Figure 3.
Panel A compares DF, OI, FI and ShEn in the HF PLA and LAA. Panel B compares heterogeneity (SD) of DF, OI, FI and ShEn in the HF PLA and LAA.

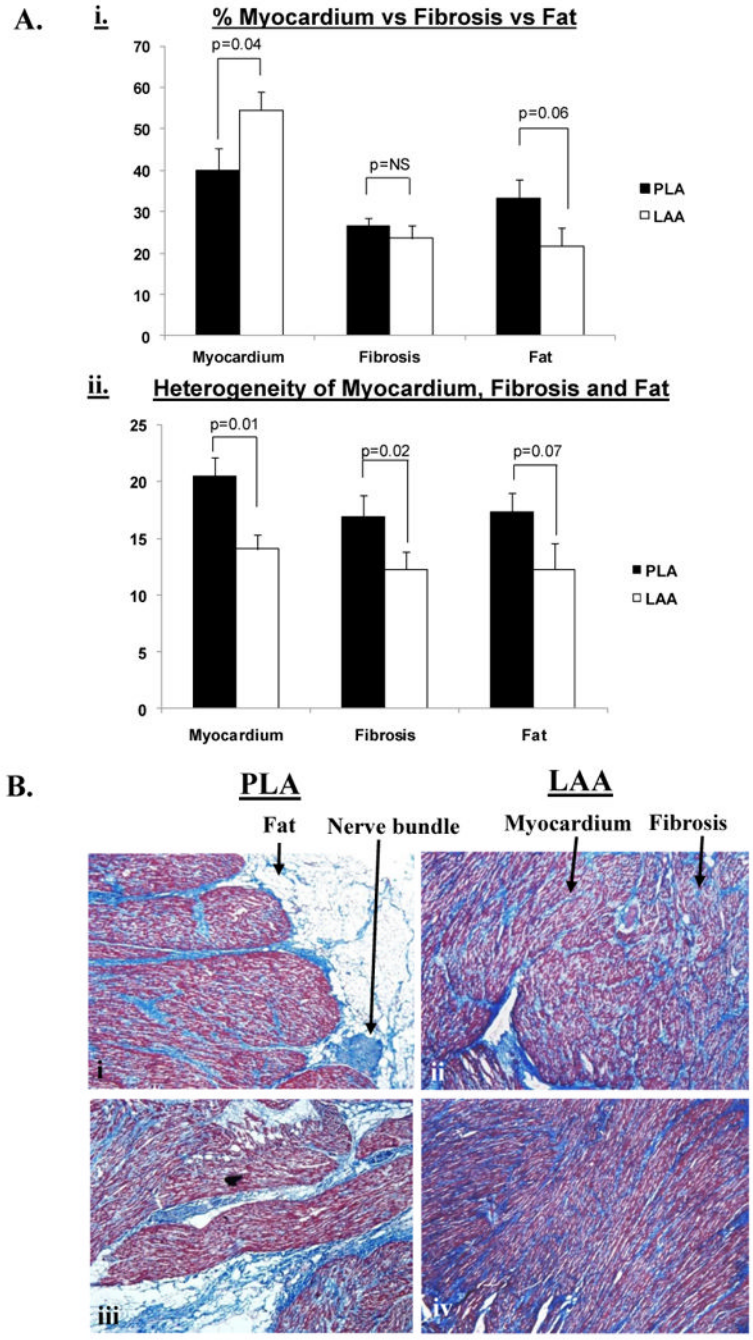

Figure 4.

Panel A, subpanel i shows the relative percentages of fat, fibrosis and myocardium in the PLA vs. LAA in HF dogs. Panel A, subpanel ii shows the heterogeneity of fat, fibrosis and myocardium in the PLA and LAA of HF dogs. Panel B, subpanels i - iv show individual sections (4X) from the PLA (subpanels i and iii) and LAA (subpanels ii and iv) respectively, highlighting that: a) there is significantly more fat in the PLA than the LAA and b) fibrosis, fat and myocardium are all more heterogeneously distributed in the PLA than the LAA. In addition, subpanel i demonstrates a typical nerve trunk in the PLA.

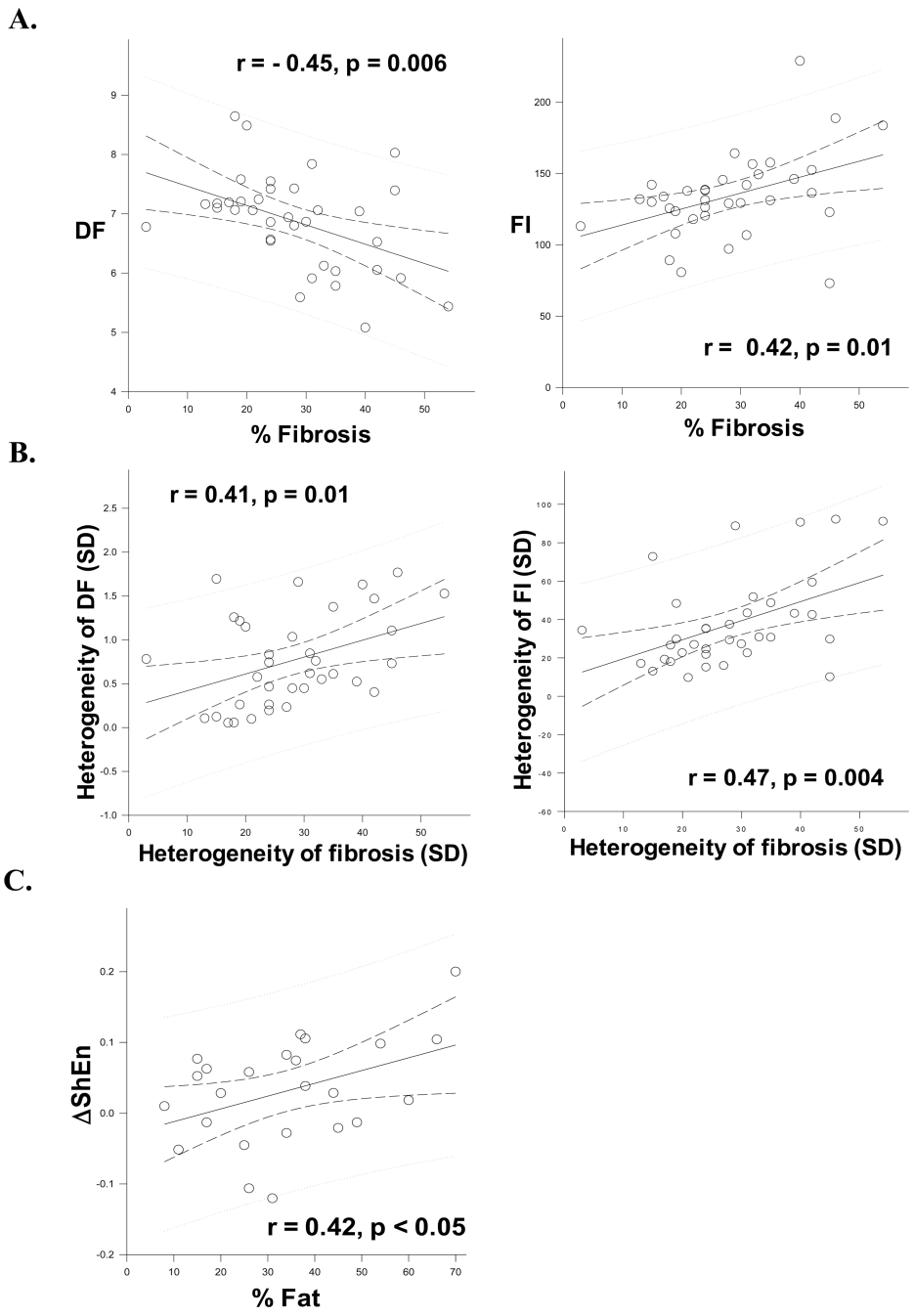

Figure 5.

Panel A, subpanels i and ii shows the correlation between % fibrosis in the PLA and DF and FI respectively. Panel B shows the correlation between heterogeneity of fibrosis and heterogeneity of DF and FI (subpanels i and ii respectively). Panel C shows the correlation between change in ShEn (ΔShEn) with autonomic blockade and % fat in the PLA.

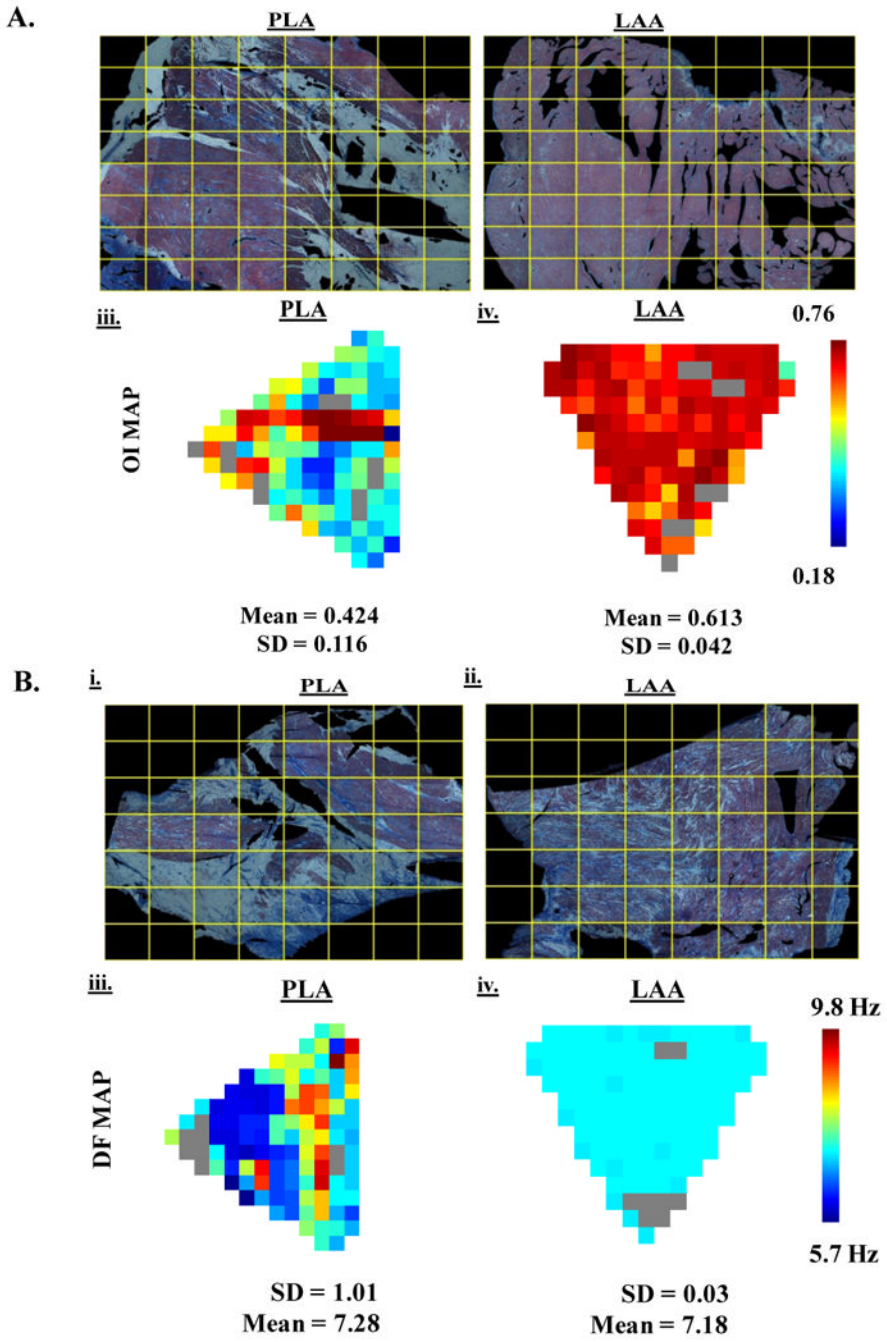

Figure 6.

Panel A shows an example of a PLA (subpanel i) and LAA section (subpanel ii) from one animal. Subpanel iii and iv shows the corresponding OI of the AF signals recorded each of these regions, respectively. Panel B shows an example of a PLA (subpanel i) and LAA section (subpanel ii) from one animal. Subpanel iii and iv shows the corresponding DF of the AF signals recorded each of these regions, respectively. See text for discussion.

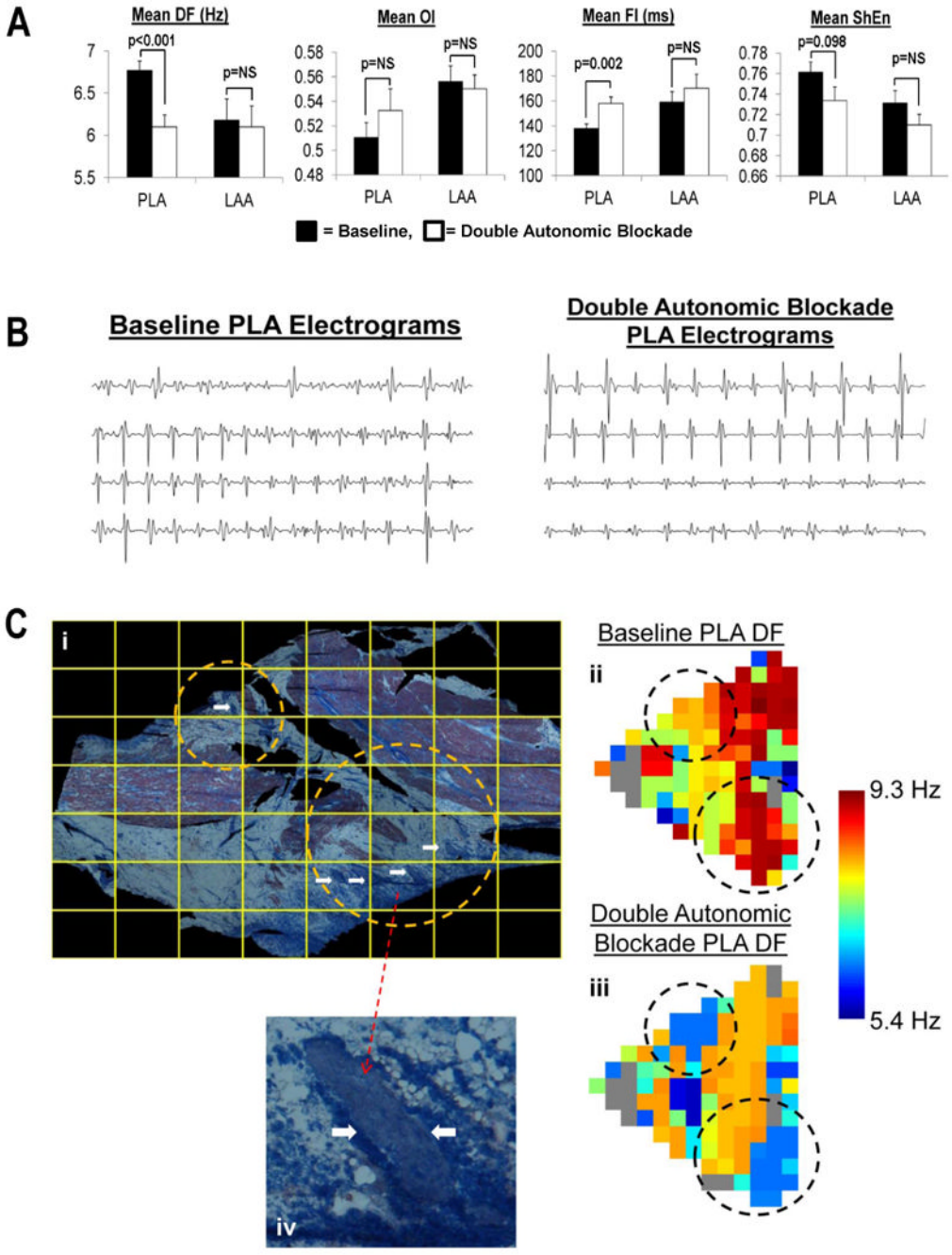

Figure 7.

Panel A shows the effects of autonomic blockade in the PLA and LAA on DF, OI, FI and ShEn. Panel B shows examples of PLA EGMs before and after double autonomic blockade. Subpanel i of Panel C shows the entire PLA section being mapped. The circles highlight areas containing several large nerve trunks indicated by white arrows.Subpanels ii and iii show the DF of an AF episode recorded at baseline and in the presence of double autonomic blockade, respectively. As shown, autonomic blockade resulted in lower DFs in both the upper circle (from roughly 8 to 6 Hz) and in the lower circle (from roughly 9 to 6 Hz). Subpanel iv shows a magnified view of a single nerve trunk seen in the lower encircled area in subpanel i.